Arch. Mech., **52**, 6, pp. 933–948, Warszawa 2000

A cracked piezoelectric material under generalized plane electromechanical impact

B. L. WANG ([1]) and N. NODA ([2])

([1]) *Center for Composite Materials, Harbin Institute of Technology, Harbin 150001, China*
e-mail: wangbl@public.hr.hl.cn

([2]) *Department of Mechanical Engineering, Shizuoka University, Hamamatsu 432-8561, Japan*

SOLUTION OF THE GENERALIZED plane deformation problem of a piezoelectric material strip with a crack is proposed. Laplace and Fourier transforms are used to reduce the problem to the solution of singular integral equations in the Laplace transform plane. Laplace inversion yields the results in the time domain. This analysis yields six independent stress and three electric displacement components. The model is general enough to account for arbitrary polarization direction, under transient or steady state load, for any mechanical or electrical mode of cracking. Numerical solutions for a piezoelectric material strip under electromechanical impact are illustrated. The influences of strip thickness and crack position on time-dependent crack tip fields are investigated. The results show that the transient electric displacement loads can increase or reduce the stress intensity factors at different time, dependent on the applied electric displacement load direction.

Key Words: Piezoelectric materials, fracture mechanics, crack, stress intensity factor, impact load.

1. Introduction

IN DESIGNING THE PIEZOELECTRIC materials, one must take into consideration imperfections, such as crack, that are often preexisting or are generated by external impact forces during the service life. The existence of a crack can significantly change the dynamic response of piezoelectric materials and structures. A significant amount of research has been performed in modeling the crack in piezoelectric materials [1 – 5]. In particular, the dynamic stress intensity factor of a cracked dielectric medium in a uniform electric field was studied by SHINDO and his colleagues [6]. NARITA and SHINDO [7] investigated the scattering of Love waves by a surface-breaking cracks in a piezoelectric layer over an elastic half plane, while the crack is normal to the interface. The anti-plane shear crack growth rate of a piezoelectric ceramic body with finite width [8], and the dynamic bending of

a symmetric piezoelectric laminated plate with a through crack [9] were investigated by NARITA and SHINDO. More recently, the electroelastic problem for a piezoelectric layer with an anti-plane shear crack connected with two elastic half-planes [10], and the central crack problem in a finite piezoelectric strip [11] have been systematically studied.

In this paper, the Griffith crack in a piezoelectric material is considered with the polarization direction perpendicular to crack plane or parallel to crack plane. Dynamic loading is analyzed by using Laplace transform. The Fourier transform is used to handle the space variable. Stress and electric displacement intensity factors are determined for different crack length and crack position under different fracture mode.

2. Solutions of the crack problem

Field equations for piezoelectric materials subjected to mechanical and electrical fields can be written as

$$\sigma_{ij} = c_{ijkl}u_{k,l} + e_{lij}\phi_{,l}, \qquad D_i = e_{ikl}u_{k,l} - \in_{i,l}\phi_{,l}, \tag{2.1}$$

$$\sigma_{ij,j} = \rho\partial^2 u_i/\partial t^2, \qquad D_{i,i} = 0, \tag{2.2}$$

where σ_{ij}, u_i, D_i, and ϕ are stresses, displacements, electric displacements, and electric potential, respectively; c_{ijkl}, e_{ijk}, $\in_{il}$, and ρ are elastic constants, piezoelectric constants, dielectric permittivities, and density, respectively; t is time variable, and a comma indicates partial derivation. The electric field, E_i, is related to the electric potential, ϕ : $E_i = -\phi_{,i}$.

Inserting (2.2) into (2.1) and applying the Laplace transform with respect to time t, we have

$$c_{ijkl}u^*_{k,lj} + e_{lij}\phi^*_{,lj} = \rho p^2 u^*_i, \quad e_{ikl}u^*_{k,li} - \in_{il}\phi^*_{,li} = 0, \tag{2.3}$$

where "p" is the Laplace transform parameter. The quantities with superscript "*" denote the Laplace transform.

In the following, unless it is declared, the superscript "*" will be omitted for simplicity. Generalized plane deformation means that the field variable u_i and ϕ are functions of x_1 and x_2 only. Assume that the piezoelectric medium is infinite along the x_1 axis. We look for a solution to (2.3) of the form

$$u_k = \frac{1}{2\pi}\int_{-\infty}^{\infty} A_k(s)F(s)e^{|s|\lambda x_2}e^{-isx_1}ds, \tag{2.4}$$

$$\phi = \frac{1}{2\pi} \int_{-\infty}^{\infty} A_4(s) F(s) e^{|s|\lambda x_2} e^{-isx_1} ds, \tag{2.5}$$

where $i = \sqrt{-1}$, $F(s)$ is an unknown function to be determined. Substituting (2.4) and (2.5) into (2.1) and then into (2.3), we obtain

$$\begin{bmatrix} \Theta_{jk} & \Theta_j \\ \Theta_k & \Theta_0 \end{bmatrix} \begin{Bmatrix} A_j \\ A_4 \end{Bmatrix} = 0, \tag{2.6}$$

where j and k take the values 1, 2, and 3, and

$$\begin{aligned} \Theta_{jk} &= -c_{j1k1} - \operatorname{sgn}(s) i(c_{j1k2} + c_{j2k1})\lambda + c_{j2k2}\lambda^2 - \delta_{jk}\rho p^2/s^2, \\ \Theta_j &= -e_{1j1} - \operatorname{sgn}(s) i(e_{1j2} + e_{2j1})\lambda + e_{2j2}\lambda^2, \\ \Theta_0 &= \epsilon_{11} + \operatorname{sgn}(s) i(\epsilon_{12} + \epsilon_{21})\lambda - \epsilon_{22}\lambda^2. \end{aligned}$$

Equation (2.6) is an eigenvalue problem consisting of four equations, a nontrivial set (A_1, A_2, A_3, A_4) exists if λ is a root of the determinant. The eight roots for λ, form four conjugate pairs. In terms of these eigenvalues, a general expression for the displacements and electric potential can be written as

$$\{V(x_1, x_2)\} = \frac{1}{2\pi} \int_{-\infty}^{\infty} [A(x_2)] \{F(s)\} e^{-isx_1} ds, \tag{2.7}$$

where

$$\{V(x_1, x_2)\} = \begin{Bmatrix} u_k \\ \phi \end{Bmatrix}, \qquad k = 1, 2, 3,$$

$$[A(x_2)] = \begin{bmatrix} A_{k\alpha} e^{|s|\lambda_\alpha x_2} \\ A_{4\alpha} e^{|s|\lambda_\alpha x_2} \end{bmatrix}, \quad \{F(s)\} = \{F_\alpha\}^T, \quad \alpha = 1, ..., 8.$$

Define a new vector, $\{t_2\}$, as given by

$$\{t_2(x_1, x_2)\} = (\sigma_{21}\ \sigma_{22}\ \sigma_{23}\ D_2)^T.$$

We can obtain the following expression by using (2.1) and (2.7):

$$\{t_2(x_1, x_2)\} = \frac{1}{2\pi} \int_{-\infty}^{\infty} [B_2] \{F\} s e^{-isx_1} ds, \tag{2.8}$$

where $[B_2(x_2)]$ is a 4×8 matrix.

3. The crack problem

Consider a piezoelectric medium of height h, see Fig. 1. The body contains a crack of length $2a$ lying along x_1 axis. Let $\{t_{20}(x)\}$ represent $\{t_2(x,0)\}$, and the superscripts (1) and (2) refer to the quantities associated with the materials occupying the lower and upper parts, respectively. The initial displacement, velocities and electric potential are zero. The boundary conditions are assumed to have the following forms:

$$\begin{aligned} \{t_2(x,-h^{(1)})\} &= \{t_{10}(x,t)\}, \\ \{t_2(x,h^{(2)})\} &= \{t_{30}(x,t)\}, \\ \{t_{20}(x)\} &= \{t_0(x,t)\}, \qquad -a < x < a. \end{aligned}$$

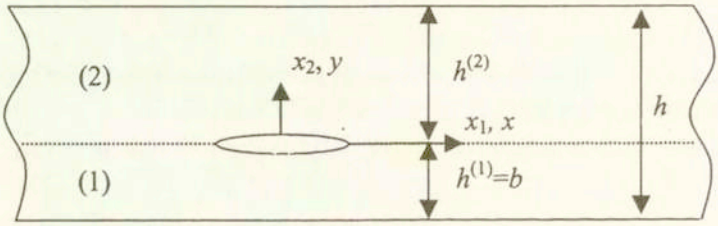

FIG. 1. A crack in a piezoelectric material strip: geometries and coordinates.

Suppose the Laplace transforms of $\{t_{10}\}$, $\{t_{30}\}$, and $\{t_{20}\}$ are $\{t_{10}^*\}$, $\{t_{30}^*\}$, and $\{t_{20}^*\}$, respectively. The unknown vector $\{F\}$ can be expressed in terms of $\{t_{10}^*\}$, $\{t_{20}^*\}$ and $\{t_{30}^*\}$ by applying the inverse Fourier transform to Eq. (2.8), i.e.,

$$\{F^{(2)}(s)\} = \frac{1}{s}\left[B^{(2)}\right]^{-1} \int_{-\infty}^{\infty} \begin{Bmatrix} t_{30}^*(x) \\ t_{20}^*(x) \end{Bmatrix} e^{isx}dx, \tag{3.1}$$

$$\{F^{(1)}(s)\} = \frac{1}{s}\left[B^{(1)}\right]^{-1} \int_{-\infty}^{\infty} \begin{Bmatrix} t_{20}^*(x) \\ t_{10}^*(x) \end{Bmatrix} e^{isx}dx, \tag{3.2}$$

where

$$[B^{(2)}] = \begin{bmatrix} B_2^{(2)}(h^{(2)}) \\ B_2^{(2)}(0) \end{bmatrix}, \quad [B^{(1)}] = \begin{bmatrix} B_2^{(1)}(0) \\ B_2^{(1)}(-h^{(1)}) \end{bmatrix}.$$

Substituting (3.1) and (3.2) back into (2.7), we have

$$\{V^{(1)}(r,y)\} = \frac{1}{2\pi}\int_{-\infty}^{\infty}\frac{1}{s}[D_1^{(1)}(y)\ D_2^{(1)}(y)]\int_{-\infty}^{\infty}\begin{Bmatrix} t_{20}^*(x) \\ t_{10}^*(x)\end{Bmatrix} e^{isx}dxe^{-isr}ds, \tag{3.3}$$

$$\{V^{(2)}(r,y)\} = \frac{1}{2\pi}\int_{-\infty}^{\infty}\frac{1}{s}[D_1^{(2)}(y)\ D_2^{(2)}(y)]\int_{-\infty}^{\infty}\begin{Bmatrix} t_{30}^*(x) \\ t_{20}^*(x)\end{Bmatrix} e^{isx}dxe^{-isr}ds. \tag{3.4}$$

where $[D_1^{(1)}]$, $[D_2^{(1)}]$, $[D_1^{(2)}]$, and $[D_2^{(2)}]$ are 4×4 matrices:

$$[D_1^{(1)}(y)\ \ D_2^{(1)}(y)] = [A^{(1)}(y)][B^{(1)}]^{-1},$$

$$[D_1^{(2)}(y)\ \ D_2^{(2)}(y)] = [A^{(2)}(y)][B^{(2)}]^{-1}.$$

Introduce the electromechanical dislocation density function $\{d\}$ along the crack faces as

$$\{d(x)\} = \partial(\{V^{(2)}(x,0)\} - \{V^{(1)}(x,0)\})/\partial x. \tag{3.5}$$

Equations (3.3) and (3.4) can be used to give

$$\{d(r)\} = \frac{i}{2\pi}\int_{-\infty}^{\infty}\left([L]\int_{-\infty}^{\infty}\{t_{10}^*\}e^{isx}dx + [M]\int_{-\infty}^{\infty}\{t_{20}^*\}e^{isx}dx + [N]\int_{-\infty}^{\infty}\{t_{30}^*\}e^{isx}dx\right)e^{-isr}ds, \tag{3.6}$$

where

$$[L(s)] = [D_2^{(1)}(0)],\quad [M(s)] = [D_1^{(1)}(0)] - [D_2^{(2)}(0)],\quad [N(s)] = -[D_1^{(2)}(0)].$$

Solving $\{t_{20}^*(x)\}$ from Eq. (3.6), we have

$$\{t_{20}^*(x)\} = \int_{-a}^{a}[K_1(x,r)]\{d(r)\}dr - \{t_b(x)\}, \tag{3.7}$$

where

$$[K_1(x,r)] = \frac{1}{2\pi i}\int_{-\infty}^{\infty}[M(s)]^{-1}e^{is(r-x)}ds, \tag{3.8}$$

$$\{t_b(x)\} = \frac{1}{2\pi}\int_{-\infty}^{\infty}[M]^{-1}\left([L]\int_{-\infty}^{\infty}\{t_{10}^*\}e^{isr}dr + [N]\int_{-\infty}^{\infty}\{t_{30}^*\}e^{isr}dr\right)e^{-isx}ds. \tag{3.9}$$

Thus $\{d\}$ is the only unknown vector in the problem which may be determined from the crack faces boundary condition. The singular behavior of the kernel $[K_1(x,r)]$ may be obtained from the asymptotic analysis of the integral in (3.8). Observe that as s tends to infinity, $[M(s)]$ tends to $\mathrm{sgn}(s)[M(\infty)]$. It can be deduced from (3.8) that

$$[K_1(x,r)] = \frac{1}{\pi}\frac{[M(\infty)]^{-1}}{r-x} + [\Lambda(x,r)],$$

$$[\Lambda(x,r)] = \frac{1}{2\pi i}\int_{-\infty}^{\infty}\left([M(s)]^{-1} - \mathrm{sgn}(s)[M(\infty)]^{-1}\right)e^{is(r-x)}ds.$$

In view of the uniform convergence, the function defined by

$$\{t_{0b}(x)\} = \int_{-a}^{a}[\Lambda(x,r)]\{d(r)\}dr,$$

is bounded in the closed interval $-a \le x \le a$. Observe that (3.7) gives $\{t_{20}^*(x)\}$ outside as well as inside of the crack. For the latter, (3.7) may be expressed as

$$\{t_0^*(x)\} = \frac{[M(\infty)]^{-1}}{\pi}\int_{-a}^{a}\frac{\{d(r)\}}{r-x}dr + \int_{-a}^{a}[\Lambda(x,r)]\{d(r)\}dr - \{t_b(x)\}, \tag{3.10}$$

where $\{t_0^*(x)\}$ is the Laplace transform of $\{t_0(x,t)\}$.

A numerical technique to solve singular integral equations of the above form has been developed by ERDOGAN and GUPTA [12], where a weighted residual technique is employed to reduce the singular integral equations to a set of algebraic equations in unknown coefficients of Chebychev polynomials of the first kind. This method was also used by WANG [13] for the fracture analysis of the nonhomogeneous materials. Note that the solution for $\{d\}$ has the form

$$\{d(r)\} = \sum_{m=1}^{M}\{C^m\}T_m(\bar{r})/\sqrt{1-\bar{r}^2}, \tag{3.11}$$

where $\bar{r} = r/a$, $T_m(\bar{r})$ is the Chebychev polynomials of the first kind. Upon evaluating $\{C^m\}$ from (3.10) and (3.11), the displacements and electric potential differences between the crack faces can be evaluated from Eqs. (3.5) and (3.11) as

$$\{\Delta(r)\} = -a \sum_{m=1}^{\infty} \{C^m\} \frac{\sin(m \, ar\cos\bar{r})}{m}, \qquad \bar{r} < 1.$$

The stress and electric displacement intensity factors, i.e., in-plane normal traction (Mode I), in-plane shear (Mode II), anti-plane shear (Mode III), in-plane electric displacement (Mode IV), $\{K\} = \{K_{\mathrm{II}} \; K_{\mathrm{I}} \; K_{\mathrm{III}} \; K_{\mathrm{IV}}\}^T$ can be calculated by

$$\{K\} = \left(\sqrt{2[(-a) - x]}\right)_{x \to (a)^-} \{t^*_{20}(x)\}$$

$$= [M(\infty)]^{-1} \sqrt{a} \sum_{m=1}^{M} (-1)^m \{C^m\}, \tag{3.12}$$

for the left-hand side crack-tip, and

$$\{K\} = \left(\sqrt{2[x - a]}\right)_{x \to (a)^+} \{t^*_{20}(x)\} = -[M(\infty)]^{-1} \sqrt{a} \sum_{m=1}^{M} \{C^m\}, \tag{3.13}$$

for the right-hand side crack-tip.

Once the elastic and electric fields in Laplace transform plane are obtained, the corresponding values in the time domain are given by the Laplace inversion. The numerical Laplace inversion methods used here is due to DURBIN [14], a study of Durbin's method has been made by NARAYANAN and BESKOS [15].

Suppose that $F^*(p)$ is the Laplace transform of the function $F(t)$, then $\lim\limits_{p \to 0} pF^*(p) = \lim\limits_{t \to \infty} F(t)$. Therefore, we can obtain the static solutions of the field intensity factors in the physical space using (3.12) and (3.13).

4. The special cases

The polarization direction of the piezoelectric material is conventionally chosen as the x_3 direction. Constitutive relations for piezoelectric ceramics polarized along x_3 direction exhibiting transversely isotropic behavior (hexagonal symmetry) can be written in the following form:

$$\begin{Bmatrix} \sigma_{11} \\ \sigma_{22} \\ \sigma_{33} \\ \sigma_{23} \\ \sigma_{31} \\ \sigma_{12} \end{Bmatrix} = \begin{bmatrix} c_{11} & c_{12} & c_{13} & 0 & 0 & 0 \\ c_{12} & c_{22} & c_{13} & 0 & 0 & 0 \\ c_{13} & c_{13} & c_{33} & 0 & 0 & 0 \\ 0 & 0 & 0 & c_{44} & 0 & 0 \\ 0 & 0 & 0 & 0 & c_{44} & 0 \\ 0 & 0 & 0 & 0 & 0 & c_{66} \end{bmatrix} \begin{Bmatrix} \varepsilon_{11} \\ \varepsilon_{22} \\ \varepsilon_{33} \\ \varepsilon_{23} \\ \varepsilon_{31} \\ \varepsilon_{12} \end{Bmatrix}$$

$$- \begin{bmatrix} 0 & 0 & e_{31} \\ 0 & 0 & e_{31} \\ 0 & 0 & e_{33} \\ 0 & e_{15} & 0 \\ e_{15} & 0 & 0 \\ 0 & 0 & 0 \end{bmatrix} \begin{Bmatrix} E_1 \\ E_2 \\ E_3 \end{Bmatrix},$$

$$\begin{Bmatrix} D_1 \\ D_2 \\ D_3 \end{Bmatrix} = \begin{bmatrix} 0 & 0 & 0 & 0 & e_{15} & 0 \\ 0 & 0 & 0 & e_{15} & 0 & 0 \\ e_{31} & e_{31} & e_{33} & 0 & 0 & 0 \end{bmatrix} \begin{Bmatrix} \varepsilon_{11} \\ \varepsilon_{22} \\ \varepsilon_{33} \\ \varepsilon_{23} \\ \varepsilon_{31} \\ \varepsilon_{12} \end{Bmatrix}$$

$$+ \begin{bmatrix} \in_{11} & 0 & 0 \\ 0 & \in_{11} & 0 \\ 0 & 0 & \in_{33} \end{bmatrix} \begin{Bmatrix} E_1 \\ E_2 \\ E_3 \end{Bmatrix}.$$

Assume that the field variable u, v, and ϕ are functions of x and y only. The model described above is general enough to treat the fracture problems for piezoelectric materials with polarization axis along arbitrary direction. For the crack configuration and the orthogonal coordinate system shown in Fig. 1, we can obtain some special mechanical and electrical responses in any of the three directions.

CASE 1. Polarization axis perpendicular to the x-y plane

The in-plane displacements are governed by the equations

$$c_{11}\frac{\partial^2 u}{\partial x^2} + (c_{12} + c_{66})\frac{\partial^2 v}{\partial x \partial y} + c_{66}\frac{\partial^2 u}{\partial y^2} = \rho\frac{\partial^2 u}{\partial t^2},$$

$$c_{66}\frac{\partial^2 v}{\partial x^2} + (c_{12} + c_{66})\frac{\partial^2 u}{\partial x \partial y} + c_{22}\frac{\partial^2 v}{\partial y^2} = \rho\frac{\partial^2 v}{\partial t^2}.$$

This is a plane elastic crack problem. The piezoelectric effect has no influence on in-plane displacements and stresses.

The electrical potential and out-of-plane displacement w are governed by

$$c_{44}\left(\frac{\partial^2 w}{\partial x^2}+\frac{\partial^2 w}{\partial y^2}\right)+e_{15}\left(\frac{\partial^2 \phi}{\partial x^2}+\frac{\partial^2 \phi}{\partial y^2}\right)=\rho\frac{\partial^2 w}{\partial t^2},$$

$$e_{15}\left(\frac{\partial^2 w}{\partial x^2}+\frac{\partial^2 w}{\partial y^2}\right)-\epsilon_{11}\left(\frac{\partial^2 \phi}{\partial x^2}+\frac{\partial^2 \phi}{\partial y^2}\right)=0.$$

The electrical potential is coupled only with the out-of-plane displacement w. This is the anti-plane electro-elastic crack problem.

CASE 2. Polarization axis along the y direction

The governing equations for in-plane displacements and electric potential are the following

$$c_{11}\frac{\partial^2 u}{\partial x^2}+c_{44}\frac{\partial^2 u}{\partial y^2}+(c_{13}+c_{44})\frac{\partial^2 v}{\partial x\partial y}+(e_{31}+e_{15})\frac{\partial^2 \phi}{\partial x\partial y}=\rho\frac{\partial^2 u}{\partial t^2},$$

$$(c_{13}+c_{44})\frac{\partial^2 u}{\partial x\partial y}+c_{44}\frac{\partial^2 v}{\partial x^2}+c_{33}\frac{\partial^2 v}{\partial y^2}+e_{15}\frac{\partial^2 \phi}{\partial x^2}+e_{33}\frac{\partial^2 \phi}{\partial y^2}=\rho\frac{\partial^2 v}{\partial t^2},$$

$$(e_{31}+e_{15})\frac{\partial^2 u}{\partial x\partial y}+e_{15}\frac{\partial^2 v}{\partial x^2}+e_{33}\frac{\partial^2 v}{\partial y^2}-\epsilon_{11}\frac{\partial^2 \phi}{\partial x^2}-\epsilon_{33}\frac{\partial^2 \phi}{\partial y^2}=0.$$

The electrical potential is coupled with in-plane displacements u and v.

The anti-plane displacement is governed by the equation

$$c_{66}\frac{\partial^2 w}{\partial x^2}+c_{44}\frac{\partial^2 w}{\partial y^2}=\rho\frac{\partial^2 w}{\partial t^2}.$$

This is an anti-plane elastic crack problem for orthotropic materials.

5. Results and discussion

We consider a PZT-5H piezoelectric ceramics strip as an example. The thickness of the medium is h. The elastic constants are $c_{11}=12.6\times10^{10}$ N/m^2, $c_{13}=8.41\times10^{10}$ N/m^2, $c_{33}=11.7\times10^{10}$ N/m^2, $c_{44}=2.3\times10^{10}$ N/m^2. The piezoelectric constants are $e_{31}=-6.5$ C/m^2, $e_{33}=23.3$ C/m^2, $e_{15}=17.44$ C/m^2. The dielectric permittivities are $\epsilon_{11}=150.3\times10^{-10}$ C/Vm, $\epsilon_{33}=130.0\times10^{-10}$ C/Vm. The mass density is $\rho=7500$ Kg/m^3. We postulate the crack faces are free from mechanical traction and are electrically insulated.

5.1. Polarization axis perpendicular to the x-y plane

This is the case of anti-plane mechanical deformation and in-plane electric

fields. Assume a sudden mechanical loading τ_0 applied to the upper and lower surfaces of the strip. It is found that the electric displacement intensity factor is zero at the crack tip. Figure 2 shows the variation of stress intensity factor K_{III} with time. The results are the same as those for homogeneous material without the piezoelectric effect. It follows that for homogeneous materials under mechanical loading, the piezoelectric effect has no influence on the stress intensity factor.

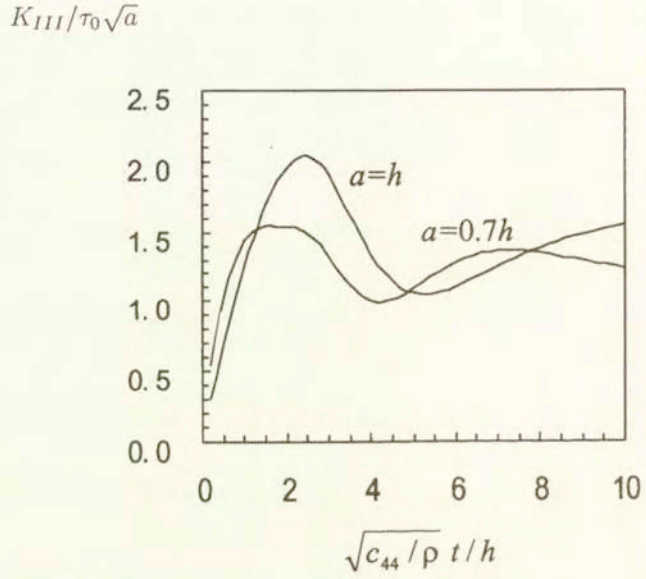

FIG. 2. Anti-plane stress intensity factor for a centrally cracked PZT-5H ceramics strip under transient mechanical load.

Assume a transient electric displacement load D_0 applied to the upper and lower surfaces of the strip. It is found that the dynamic stress intensity factors are not zero and they are plotted in Fig. 3. When time t approaches infinity the steady state stress intensity factors become zero. These results show that, differ from the static case, the transient electric displacement load can produce stress in the crack plane ahead of the crack tip.

5.2. Polarization axis along the y direction

The in-plane electrical field is coupled with in-plane displacements u and v. Assume that the upper and lower surfaces of the strip are loaded by a sudden stress σ_0 and a sudden electric displacement D_0. If the crack is located in the mid-plane of the strip, the shear stress in the plane of $y = 0$ is zero. Figures 4 and 5 show, respectively, the variation of normal stress intensity factor and electric

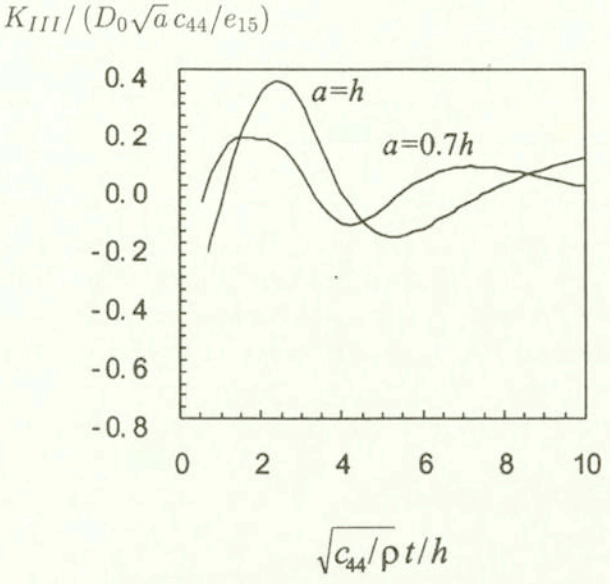

FIG. 3. Anti-plane stress intensity factor for a centrally cracked PZT-5H ceramics strip under transient electrical load.

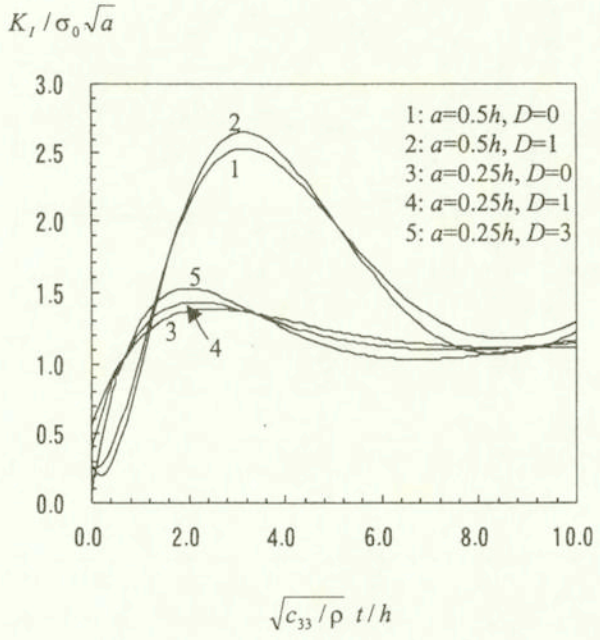

FIG. 4. Variation of normal stress intensity factor with time for different crack lengths and electric loads ($b/h = 0,5$).

displacement intensity factor with time. It is seen that as the relative thickness of the strip decreases, the field intensity factors increase. The stress intensity factors can increase or decrease with applied electric load, depending on the time t. At very early times, the presence of electric displacement load will reduce the stress intensity factors. The oppose trends are found for larger t. The presence of transient electric displacement load will always increase the peak stress intensity factor. Note that the applied electric displacement load is positive. Suppose a negative electric displacement load is applied, the transient electric displacement load will always reduce the peak stress intensity factor. This is different from the available date for piezoelectric materials under static loads. It has been shown that the steady-state stress intensity factor does not depend on the applied electric displacement load.

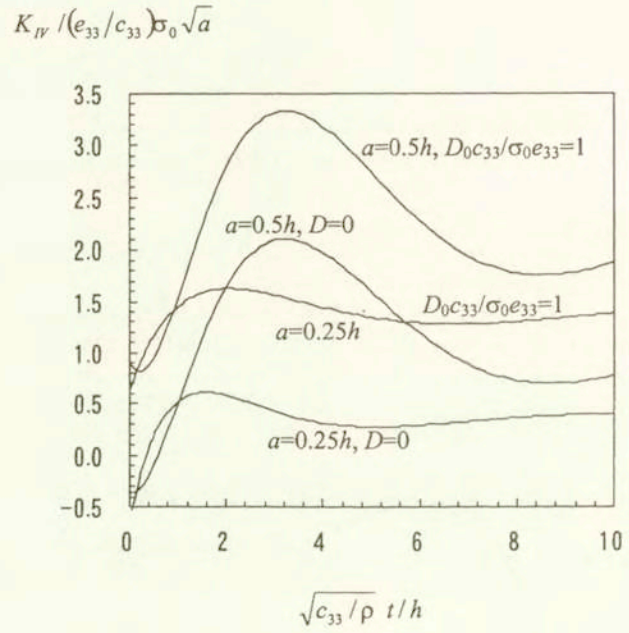

FIG. 5. Variation of electric displacement intensity factor with time for different crack lengths and electric loads ($b/h = 0.5$).

Figures 6, 7 and 8 show the influence of the crack position on the stress and electric displacement intensity factors. When the crack is located in the center of the strip, K_{II} is zero. The Mode II stress intensity factor is not zero when crack is not located in the mid-plane of the strip. As the crack approaches the surface of the strip, the field intensity factors increase quickly and the crack will more likely extend.

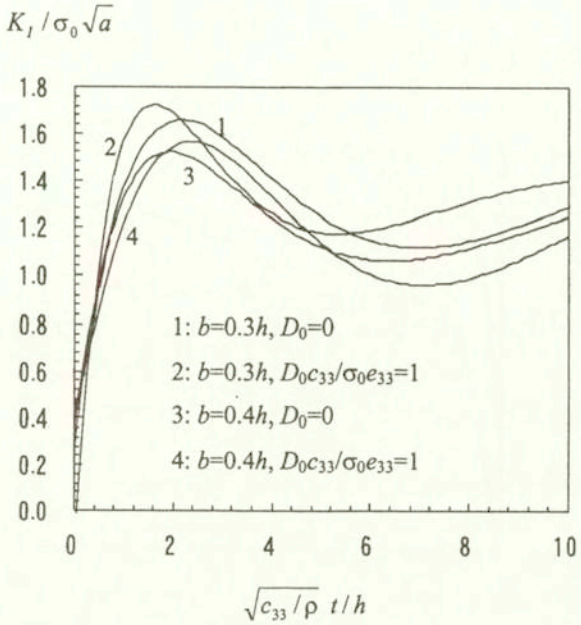

FIG. 6. Variation of normal stress intensity factor with time for different crack positions and electric loads ($a = 0.25h$).

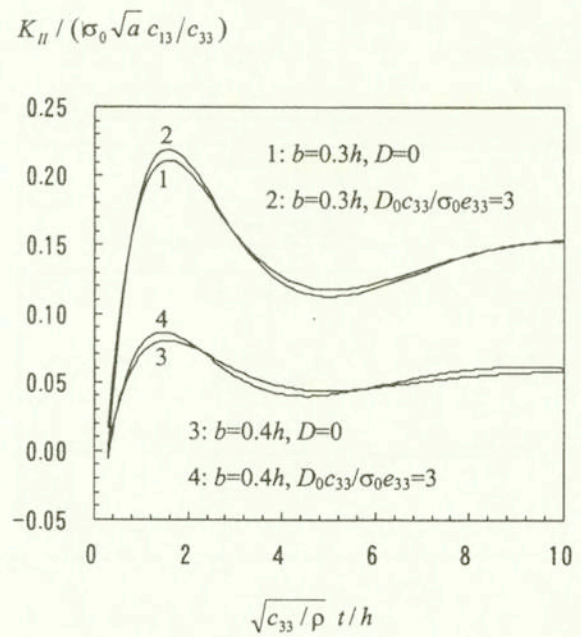

FIG. 7. Variation of shear intensity factor with time for different crack positions and electric loads ($a = 0.25h$).

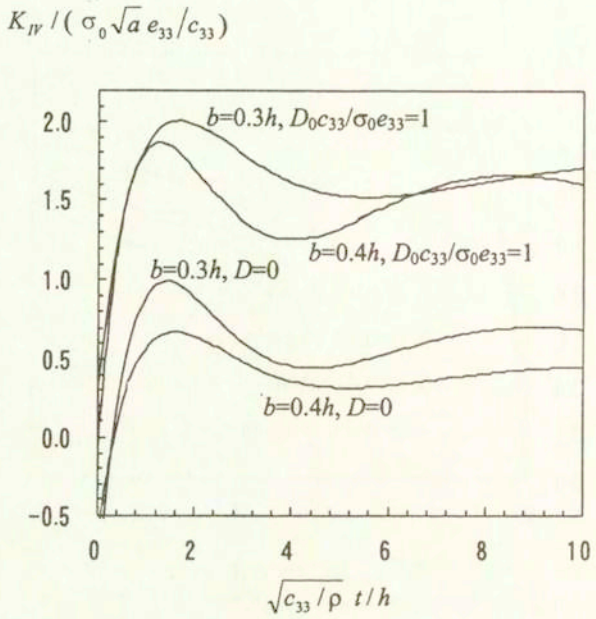

FIG. 8. Variation of electric displacement intensity factor with time for different crack positions and electric loads ($a = 0.25h$).

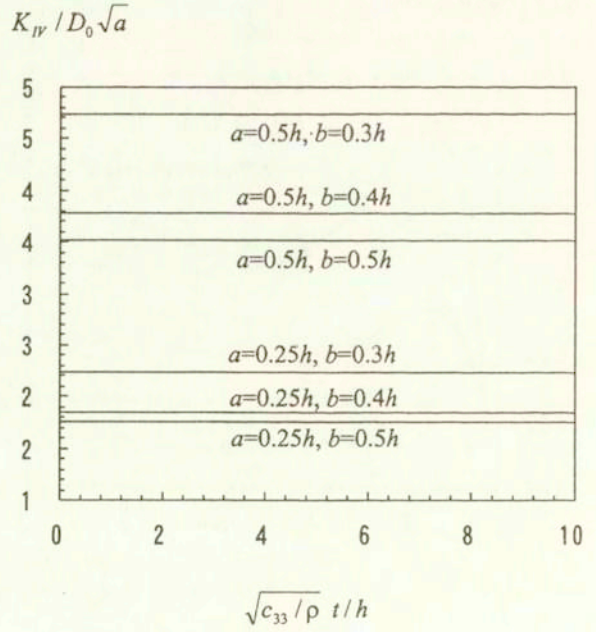

FIG. 9. Variation of electric displacement intensity factor with time (pure electric load).

Consider a pure electric displacement load D_0 applied on the surfaces of the strip. It is found that the electric displacement intensity factors are time independent as shown in Fig. 9. The same fact was also found for anti-plane crack problem.

6. Conclusion

Fracture is one of the properties that limit the use of piezoelectric materials as sensors and actuators in smart materials and structures technology. The present work focuses on the fracture mechanics analysis for finite thickness piezoelectric medium with the polarization axis along arbitrary direction. Particularly, numerical solutions for a piezoelectric material strip under in-plane and anti-plane electromechanical impacts are analyzed. It is found that as the relative length of the crack increases, the field intensities increase quickly. The crack position has a pronounced influence on field intensities ahead of the crack tip. The electric field can retard or enhance the crack tip stress intensity factors at different times, depending on the applied field displacement load direction.

Acknowledgement

B. L. Wang's work is supported by the National Science Foundation of China under grant 19902003, and by the JSPS (the Japan Society for the Promotion of Science) postdoctoral fellowship program.

References

1. Y. E. Pak, *Crack extension force in a piezoelectric material*, J. Appl. Mech., **57**, 647–653, 1990.
2. Y. E. Pak, *Linear electro-elastic fracture mechanics of piezoelectric materials*, Int. J. of Fracture, **54**, 79–100, 1992.
3. H. Sosa, *On the fracture mechanics of piezoelectric solids*, Int. J. Solids Struct., **29**, 2613–2622, 1992.
4. Z. Suo, C. M. Kuo, D. M. Barnett, J. R. Willis, *Fracture mechanics for piezoelectric ceramics*, J. Mech. and Phys. Solids, **40**, 739–765, 1992.
5. T. Y. Zhang, C. F. Qian, P. Tong, *Linear electro-elastic analysis of a cavity or a crack in a piezoelectric material*, Int. J. Solids and Struct., **35**, 2121–2149, 1998.
6. Y. Shindo, H. Katsura, W. Yan, *Dynamic stress intensity factor of a cracked dielectric medium in a uniform electric field*, Acta Mechanica, **117**, 1–10, 1996.
7. F. Narita, Y. Shindo, *Scattering of love waves by a surface-breaking crack in piezoelectric layered media*, JSME Int. J., Series A, **41**, 40–48, 1998.
8. F. Narita, Y. Shindo, *Anti-plane shear crack growth rate of piezoelectric ceramic body with finite width*, Theoretical and Applied Fracture Mechanics, **30**, 127–132, 1998.

9. Y. SHINDO, W. DOMON, F. NARITA, *Dynamic bending of a symmetric piezoelectric laminated plate with a through crack*, Theoretical and Applied Fracture Mechanics, **28**, 175–182, 1998.

10. F. NARITA, Y. SHINDO, K. WATANABE, *Anti-plane shear crack in a piezoelectric layer bonded to dissimilar half spaces*, JSME Int. J., Series A, **42**, 66–72, 1999.

11. Y. SHINDO, K. WATANABE, F. NARITA, *Electroelastic analysis of a piezoelectric ceramic strip with a central crack*, Int. J. Engng. Science, **38**, 1–19, 1999.

12. F. ERDOGAN, G. GUPTA, *On the numerical solution of singular integral equations*, Q. J. Appl. Math., **1**, 525–534, 1972.

13. B. L. WANG, J. C. HAN, S. Y. DU, *Crack problems in inhomogeneous composites subjected to dynamic loading*, Int. J. Solids Struct., **37**, 1251–1274, 2000.

14. F. DURBIN, *Numerical inversion of Laplace transforms: An efficient improvement to Duber and Abate's method*, The Computer Journal, **17**, 371–376, 1974.

15. G. V. NARAYANAN, D. E. BESKOS, *Numerical operational methods for time-dependent linear problems*, International Journal for Numerical Methods Engineering, **18**, 1829–1854, 1982.

Received March 13, 2000.